Volatility study of [C₁C₁im][NTf₂] and [C₂C₃im][NTf₂] ionic liquids

Marisa A.A. Rocha [a,*], Filipe M.S. Ribeiro [a], Bernd Schröder [b], João A.P. Coutinho [b], Luís M.N.B.F. Santos [a,*]

[a] Centro de Investigação em Química, Departamento de Química e Bioquímica, Faculdade de Ciências da Universidade do Porto, R. Campo Alegre 687, P-4169-007 Porto, Portugal
[b] CICECO, Departamento de Química, Universidade de Aveiro, 3810-193 Aveiro, Portugal

ABSTRACT

Vapor pressures of 1,3-dimethylimidazolium bis(trifluoromethylsulfonyl)imide, ([C₁C₁im][NTf₂]) and 1-ethyl-3-propylimidazolium bis(trifluoromethylsulfonyl)imide, ([C₂C₃im][NTf₂]) ionic liquids were measured as a function of temperature using a Knudsen effusion apparatus combined with a quartz crystal microbalance. Enthalpies and entropies of vaporization were derived from the fitting of vapor pressure and temperature results to the Clarke and Glew equation. [C₁C₁im][NTf₂] presents a higher enthalpy and entropy of vaporization than the neighboring members of the series. The enthalpy of vaporization of [C₂C₃im][NTf₂] lies in between the asymmetric and symmetric ionic liquid series, reflecting a decrease in the electrostatic interactions due to a decrease of the charge accessibility between the ionic pairs when the methyl group is replaced by an ethyl group. The obtained higher volatility of [C₂C₃im][NTf₂] arises from its asymmetric character, leading to an higher entropic contribution that compensates the enthalpic penalty. The border conditions ([C₁C₁im][NTf₂], [C₂C₁im][NTf₂] and [C₂C₂im][NTf₂]), topology ([C₂C₃im][NTf₂]) and symmetry/asymmetry of the ILs effect were evaluated and rationalized based on a comparative analysis of the thermodynamic properties, enthalpies and entropies of vaporization.

1. Introduction

Recently, we have reported on the (vapor + liquid) equilibrium study of the extended series of ILs, [C$_{N-1}$C₁im][NTf₂] (with N = 3 to 9, 11, and 13), were the effect of nanostructuration of the [C$_{N-1}$C₁im][NTf₂] series on the thermodynamic properties of vaporization and viscosity was highlighted [1]. In the previous work, the thermodynamic properties of vaporization presented trend shifts along the alkyl side chain length, related to a change in the molecular structure of the liquid phase around [C₆C₁im][NTf₂] [1,2]. On another recent work, the effect of the cation's topological symmetry on the thermodynamic properties of vaporization for the symmetric ILs [C$_{N/2}$C$_{N/2}$im][NTf₂], with N = 4, 6, 8, 10, 12, was reported [3]. Based on this work, it was possible to observe that the symmetry of the cation, [C$_{N/2}$C$_{N/2}$im][NTf₂], leads to higher volatilities and lower enthalpies and entropies of vaporization, when compared with the asymmetric ILs, [C$_{N-1}$C₁im][NTf₂].

The present work is an extension of the previous studies, which deals with the thermophysical properties of imidazolium based ionic liquids, ILs [1,3,4]. The vapor pressures of 1,3-dimethylimidazolium bis(trifluoromethylsulfonyl)imide, [C₁C₁im][NTf₂], and

1-ethyl-3-propylimidazolium bis(trifluoromethylsulfonyl)imide, [C₂C₃im][NTf₂], were determined at different temperatures, using a quartz microbalance Knudsen effusion apparatus [5]. Based on the previous results, the thermodynamic properties of vaporization of the ionic liquids with short alkyl chains are reported, discussed and evaluated considering the effect of the cation's symmetry and alkyl side chain length. The schematic representation of the studied imidazolium based ionic liquids is presented in figure 1.

2. Experimental

2.1. Synthesis, purification and characterization of compounds

1,3-Dimethylimidazolium bis(trifluoromethylsulfonyl)imide ([C₁C₁im][NTf₂]) has been synthesized by means of halide-free Carbonate Based Ionic Liquid Synthesis (CBILS©), of proionic/Sigma–Aldrich [6–8]. 1,3-Dimethylimidazolium hydrogen carbonate solution (∼50% in methanol: water (2:3) (Sigma–Aldrich) has been treated with an stoichiometric amount of bis(trifluoromethylsulfonyl)imide lithium salt (Sigma–Aldrich). After separating from the precipitate, the aqueous phase has been discarded. The remaining organic phase has been washed with water. After further phase separation, remaining water and methanol has been removed in vacuum, leaving [C₁C₁im][NTf₂]. The sample was characterized by ¹H-NMR (chloroform-d, δ/ppm relative to TMS): 8.86 (s, 1H),

* Corresponding authors. Tel.: +351 220 402 836; fax: +351 220 402 659.

E-mail addresses: marisa.alexandra.rocha@gmail.com (M.A.A. Rocha), lbsantos@fc.up.pt (L.M.N.B.F. Santos).
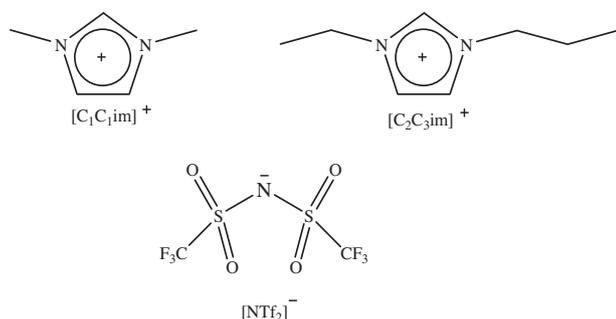
FIGURE 1. Schematic representation of the studied ionic liquids.

7.25 (d, 2H), 3.97 (s, 6H). 1-Ethyl-3-propylimidazolium bis(trifluoromethylsulfonyl)imide [C$_2$C$_3$im][NTf$_2$] was acquired from IOLITEC with a stated purity of better than 99%. The studied ionic liquids were dried under reduced pressure (<10 Pa) and stirred constantly for a minimum of 48 h at 353 K, in order to reduce the presence of water or other volatile contents. Karl Fischer titration of the degassed samples revealed less than 100 ppm of water.

2.2. Quartz crystal microbalance Knudsen effusion apparatus

The vapor pressures of the two ionic liquids were measured as a function of temperature using a Knudsen effusion apparatus combined with a quartz crystal microbalance, KEQCM [5]. This apparatus comprises two mass loss detection techniques, gravimetric and quartz crystal microbalance, which enables the decrease of effusion times and the sample size. Furthermore, the combination of two mass loss determination techniques permits the instrument to measure vapor pressures from 0.005 Pa up to 1 Pa. The temperature is controlled within a temperature fluctuation of $\pm(1 \cdot 10^{-2})$ K, measured with a resolution better than $1 \cdot 10^{-3}$ K and along the working temperature range, the overall uncertainty is better than $\pm(2 \cdot 10^{-2})$ K. The vapor pressure data obtained with this apparatus for the ionic liquid have a typical pressure dependent uncertainty of 1% to 5% [5]. The relative atomic masses used were those recommended by the IUPAC Commission in 2007 [9]. The claimed uncertainty is done based on the overall results obtained from the fitting of the Clarke and Glew equation and is valid for the middle of the experimental p, T region.

3. Results and discussion

The vapor pressures of the studied imidazolium based ionic liquids were measured at several temperatures, using the Knudsen effusion apparatus combined with a quartz crystal microbalance. The experimental vapor pressures data are listed in table 1 and

depicted in graphical representation as $\ln(p/\text{Pa}) = f[(1/T)/\text{K}^{-1}]$ in figure 2.

The experimental vapor pressures data as a function of the temperature were fitted using the Clarke and Glew equation (1) [10]:

$$R \cdot \ln\left[\frac{p(T)}{p^o}\right] = -\frac{\Delta_l^g G_m^o(\theta)}{\theta} + \Delta_l^g H_m^o(\theta) \cdot \left(\frac{1}{\theta} - \frac{1}{T}\right) + \Delta_l^g C_{p,m}^o$$
$$\cdot \left[\frac{\theta}{T} - 1 + \ln\left(\frac{T}{\theta}\right)\right], \qquad (1)$$

where $p(T)$ is the vapor pressure at the temperature T, p^o is the standard pressure ($p^o = 10^5$ Pa), θ is a selected reference temperature, R is the gas constant ($R = 8.3144621$ J $\cdot$ K^{-1} $\cdot$ mol^{-1}) [11], $\Delta_l^g G_m^o$ is the standard molar Gibbs energy of vaporization, $\Delta_l^g H_m^o$ is the standard molar enthalpy of vaporization, and $\Delta_l^g C_{p,m}^o$ is the difference between the heat capacities of the gaseous and of the liquid phases [$\Delta_l^g C_{p,m}^o = C_{p,m}^o(g) - C_{p,m}^o(l)$]. The values of $\Delta_l^g C_{p,m}^o$ were estimated for the same temperature, $T = 388$ K (mean temperature between 298.15 K and the working temperature interval), based on linear correlation of the literature values for $C_{p,m}^o(l)$ and $C_{p,m}^o(g)$ [12–15] as a function of the cation's alkyl chain length, using previously described methodology [1]. Considering the values of $\Delta_l^g C_{p,m}^o$, the
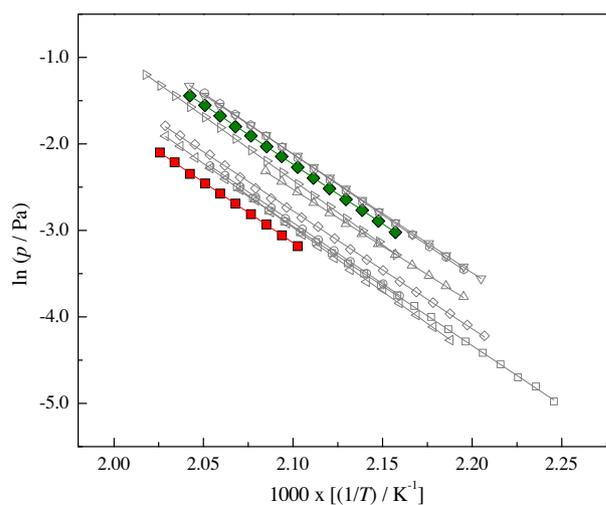

FIGURE 2. Plot of $\ln(p/\text{Pa}) = f[(1/T)/\text{K}^{-1}]$ for the studied ionic liquid: ■ (red) – [C$_1$C$_1$im][NTf$_2$]; ◆ (green) – [C$_2$C$_3$im][NTf$_2$]. Rocha *et al.* [1]: □ (gray) – [C$_2$C$_1$-im][NTf$_2$]; ◇ (gray) – [C$_3$C$_1$im][NTf$_2$]; ○ (gray) – [C$_4$C$_1$im][NTf$_2$]; ◁ (gray) – [C$_5$C$_1$im][NTf$_2$]. Rocha *et al.* [3]: △ (gray) – [C$_2$C$_2$im][NTf$_2$]; ▽ (gray) – [C$_3$C$_3$-im][NTf$_2$]; ◯ (gray) – [C$_4$C$_4$im][NTf$_2$]; ▷ (gray) – [C$_5$C$_5$im][NTf$_2$]. (For interpretation of the references to color in this figure legend, the reader is referred to the web version of this article.)

TABLE 1
Experimental vapor pressures for the studied imidazolium based ILs, as obtained with the quartz crystal microbalance Knudsen effusion apparatus.

T/K	p/Pa	Δp/Pa	T/K	p/Pa	Δp/Pa	T/K	p/Pa	Δp/Pa
				[C$_1$C$_1$im][NTf$_2$]				
475.62	0.0415	0.0013	483.59	0.0678	−0.0002	491.67	0.1095	−0.0058
477.60	0.0470	0.0001	485.60	0.0763	−0.0005	493.68	0.1225	−0.0029
479.60	0.0533	−0.0033	487.60	0.0856	0.0034			
481.59	0.0601	−0.0018	489.62	0.0957	0.0096			
				[C$_2$C$_3$im][NTf$_2$]				
463.58	0.0486	−0.0016	473.62	0.0911	0.0051	483.60	0.1651	0.0094
465.61	0.0555	−0.0037	475.62	0.1034	0.0008	485.61	0.1872	0.0004
467.59	0.0629	−0.0015	477.63	0.1172	−0.0020	487.62	0.2112	−0.0044
469.60	0.0712	0.0016	479.56	0.1311	0.0014	489.62	0.2364	−0.0030
471.62	0.0807	0.0024	481.58	0.1487	−0.0046			

$\Delta p = p - p_{\text{calc}}$, where p_{calc} is calculated from the Clarke and Glew equation (equation (1)) with the parameters given in table 2.
Standard uncertainties, u, are $u(T) = 0.02$ K, $u(p) = (0.001 + 0.05 \cdot p)$ Pa, the 0.95 confidence level ($k \approx 2$).

TABLE 2
Parameters of Clarke and Glew equation fitted from the vapor pressure results and the derived standard ($p^o = 10^5$ Pa) molar entropy of vaporization for each studied IL at the reference temperature, θ.

T^a interval/K	θ/K	$\Delta_l^g G_m^o(\theta)$/J · mol^{-1}	$\Delta_l^g H_m^o(\theta)$/J · mol^{-1}	$\Delta_l^g S_m^o(\theta)$/J · K^{-1} · mol^{-1}	r^2	$\Delta_l^g C_{p,m}^o$ ($T = 388$ K)^b/J · K^{-1} · mol^{-1}
			$[C_1C_1im][NTf_2]$			
476 to 494	484.65^a	56,990 ± 684	116,658 ± 482	123.1 ± 1.0	0.99986	−106 ± 5
	460.00	60,092 ± 678	119,271 ± 498	128.7 ± 1.0		
	298.15	84,366 ± 1305	136,427 ± 1050	174.6 ± 2.6		
			$[C_2C_3im][NTf_2]$			
464 to 490	476.60^a	54,373 ± 327	114,523 ± 225	126.2 ± 0.5	0.99995	−121 ± 5
	460.00	56,504 ± 332	116,532 ± 239	130.5 ± 0.5		
	298.15	81,565 ± 1166	136,116 ± 920	183.0 ± 2.4		

r^2 is the linear regression coefficient.
^{a} Mean temperature.
^{b} $\Delta_l^g C_{p,m}^o$ ($T = 388$ K) estimated using the linear fitted function $[\Delta_l^g C_{p,m}^o$ ($T = 388$ K)/J · K^{-1} · mol^{-1} $= -5.40n(C) - 100.47]$ derived from fitting of the literature data of $\Delta_l^g C_{p,m}^o$ ($T = 388$ K) as a function of the cationic alkyl chain length [1].

standard ($p^o = 10^5$ Pa) molar enthalpies, entropies and Gibbs energies of vaporization at reference temperature, $T = 298.15$ K, were derived. The thermodynamic properties of vaporization at the mean temperature, $\langle T \rangle$, $T = 460$ K and at 298.15 K, derived from equation (1), are presented in table 2.

The analysis and the rationalization of the thermodynamic properties of vaporization of the studied ILs will be done taking into account the literature data for the $[C_{N-1}C_1im][NTf_2]$ ($N = 3$, 4, 5, 6) [1,16], and $[C_{N/2}C_{N/2}im][NTf_2]$ ($N = 4$, 6, 8, 10) ionic liquid series [3]. Although, the thermodynamic properties of vaporization of the extended series $[C_{N-1}C_1im][NTf_2]$ ($N = 7$, 8, 9, 11, 12) are available in the literature [1], in this work we will be only focused on imidazolium based ionic liquids of short alkyl length (C_2C_1 to C_5C_1).

The standard molar Gibbs energies, enthalpies and entropies of vaporization at reference temperatures (460 and 298.15) K, as a function of the sum of the number of carbon atoms in the two alkyl side chains of the cation, are presented in figures 3–5.
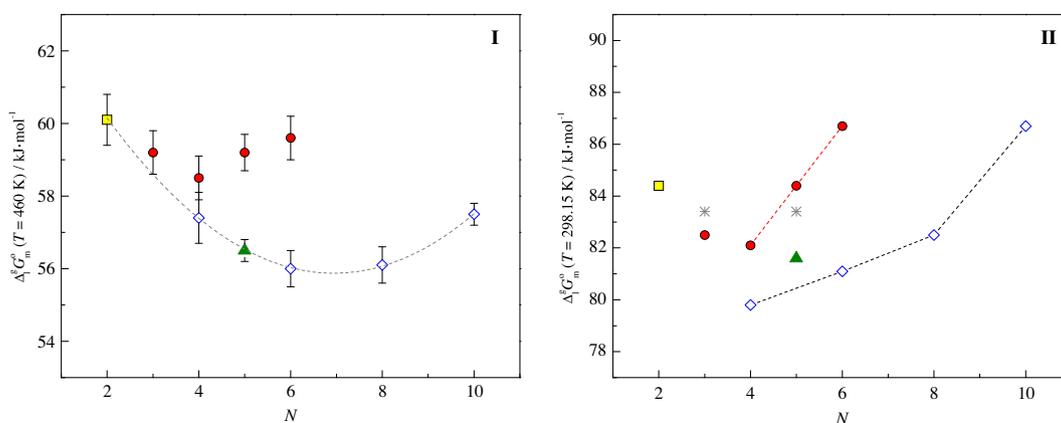

FIGURE 3. Standard ($p^o = 10^5$ Pa) molar Gibbs energy of vaporization as a function of the total number of carbons in the alkyl side chains of the cation, N: (I) $\Delta_l^g G_m^o$ ($T = 460$ K) and (II) $\Delta_l^g G_m^o$ ($T = 298.15$ K). ■ (yellow) – $[C_1C_1im][NTf_2]$; ▲ (green) – $[C_2C_3im][NTf_2]$; ● (red) – $[C_{N-1}C_1im][NTf_2]$, $N = 3$, 4, 5, 6 [1]; ◇ (blue) – $[C_{N/2}C_{N/2}im][NTf_2]$, $N = 4$, 6 [3]; ✳ (gray) – $[C_{N-1}C_1im][NTf_2]$, $N = 3$, 4 [16]. (For interpretation of the references to color in this figure legend, the reader is referred to the web version of this article.)
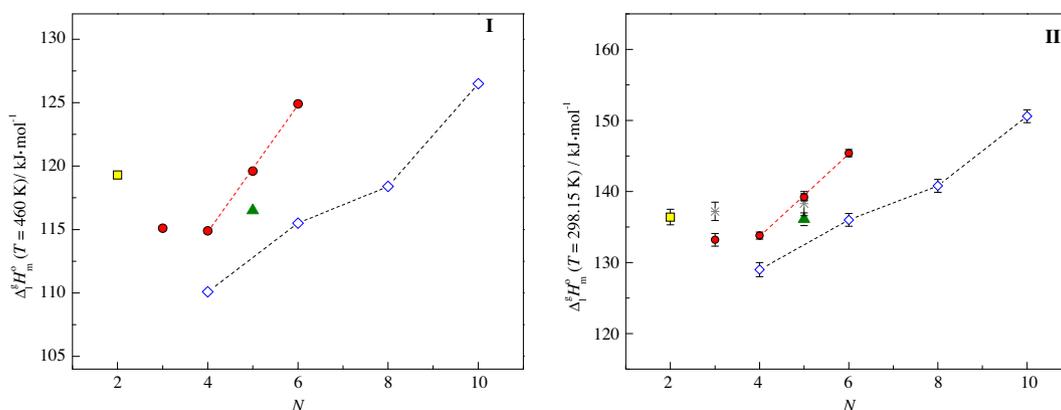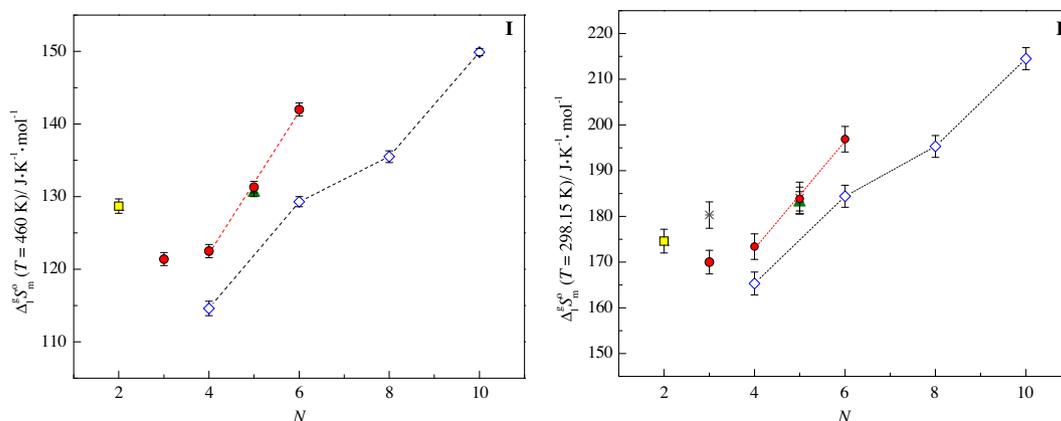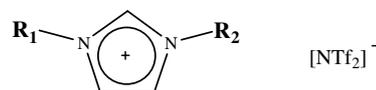

FIGURE 4. Standard ($p^o = 10^5$ Pa) molar enthalpies of vaporization as a function of the total number of carbons in the alkyl side chains of the cation, N: (I) $\Delta_l^g H_m^o$ ($T = 460$ K) and (II) $\Delta_l^g H_m^o$ ($T = 298.15$ K). ■ (yellow) – $[C_1C_1im][NTf_2]$; ▲ (green) – $[C_2C_3im][NTf_2]$; ● (red) – $[C_{N-1}C_1im][NTf_2]$, $N = 3$, 4, 5, 6 [1]; ◇ (blue) – $[C_{N/2}C_{N/2}im][NTf_2]$, $N = 4$, 6 [3]; ✳ (gray) – $[C_{N-1}C_1im][NTf_2]$, $N = 3$, 4 [16]. (For interpretation of the references to color in this figure legend, the reader is referred to the web version of this article.)

FIGURE 5. Standard ($p^o = 10^5$ Pa) molar entropy of vaporization as a function of the total number of carbons in the alkyl side chains of the cation, N: (I) $\Delta_l^g S_m^o$ ($T = 460$ K) and (II) $\Delta_l^g S_m^o$ ($T = 298.15$ K). ■ (yellow) – [C$_1$C$_1$im][NTf$_2$]; ▲ (green) – [C$_2$C$_3$im][NTf$_2$]; ● (red) – [C$_{N-1}$C$_1$im][NTf$_2$], N = 3, 4, 5, 6 [1]; ◇ (blue) – [C$_{N/2}$C$_{N/2}$im][NTf$_2$], N = 4, 6 [3]; ✳ (gray) – [C$_{N-1}$C$_1$im][NTf$_2$], N = 3, 4 [16]. (For interpretation of the references to color in this figure legend, the reader is referred to the web version of this article.)

In order to give an overview of the available data, the thermodynamic properties of vaporization published previously [1,16] were included in the graphical representations. The comparative analysis between the thermodynamic properties of vaporization obtained by our group [1] and the ones published by Zaitsau *et al.* [16] presented in the literature. Experimental vapor pressure data of ionic liquids is very scarce in the literature, and for the case of [C$_1$C$_1$im][NTf$_2$] and [C$_2$C$_3$im][NTf$_2$] no vapor pressure data was found. In order to avoid the mix-up of different levels of accuracy we will be restrict the comparison of the obtained results with literature data derived from direct experimental vapor pressures measurements.

The two studied ionic liquids and the eight imidazolium based ionic liquids published in the literature can be grouped schematically in a matrix diagram (figure 6), in which a relation between the alkyl side chains in positions 1 and 3 of the imidazolium is presented.

The asymmetric series, [C$_{N-1}$C$_1$im][NTf$_2$], is represented in the first line (red dots) and the symmetric, [C$_{N/2}$C$_{N/2}$im][NTf$_2$], as the diagonal (blue diamonds) of the diagram. [C$_1$C$_1$im][NTf$_2$] (yellow square) is the shortest alkyl side chain ionic liquid and is represented as the beginning of the symmetric and asymmetric homologous series. [C$_2$C$_3$im][NTf$_2$] (green triangle), despite being asymmetric, is located in an intermediate position in relation with the two homologous series.

A decrease of $\Delta_l^g G_m^o$, $\Delta_l^g H_m^o$ and $\Delta_l^g S_m^o$ starting from [C$_1$C$_1$im][NTf$_2$] to a minimum for the [C$_2$C$_1$im][NTf$_2$] and [C$_3$C$_1$im][NTf$_2$] (asymmetric series) and at [C$_2$C$_2$im][NTf$_2$] (symmetric series) and then increases with the alkyl chain length was observed. The expected increase of non-electrostatic interactions between ion pairs with the alkyl chain size is followed by a stronger decrease of the electrostatic potential due to the increase of the steric hindrance. This is supported and in agreement with the observed decrease of the $\Delta_l^g H_m^o$ and $\Delta_l^g S_m^o$ from [C$_1$C$_1$im][NTf$_2$] > [C$_2$C$_1$im][NTf$_2$] > [C$_2$C$_2$im][NTf$_2$]. Due to their singular molecular topology, a methyl group connected to the positions 1 and 3 of the imidazolium cation, the [C$_1$C$_1$im][NTf$_2$] presents an outlier behavior in the thermodynamic properties of vaporization. The lowest charge dispersion and the highest electrostatic ion pair interactions, which enhances the electrostatic interactions [17] between the ionic species (higher organization of the bulk). As a consequence, $\Delta_l^g H_m^o$ and $\Delta_l^g S_m^o$ is higher than for the rest of the nearest members of the series. It was found that the volatility of the ionic liquids, at $T = 460$ K, is ruled by the enthalpic contribution in which [C$_1$C$_1$im][NTf$_2$] presents

FIGURE 6. Schematic representation of the relations between the alkyl side chains of the cation of the ionic liquids under discussion.

the lower volatility compared with the other ionic liquids under discussion.

The [C$_2$C$_3$im][NTf$_2$] is located in an intermediate position between the asymmetric and symmetric ILs of the diagram. At the temperature of 460 K, their volatility fits the volatility trend of the symmetric series, however due to the higher enthalpies of vaporization and in smaller scale from the $\Delta_l^g C_{p,m}^o$ correction, at 298.15 K, the volatility of [C$_2$C$_3$im][NTf$_2$] is lower than the symmetric series. The entropy of vaporization of the [C$_2$C$_3$im][NTf$_2$] is similar to the [C$_4$C$_1$im][NTf$_2$], due to the asymmetric character of the cation. On the other hand, the enthalpy of vaporization is in between the asymmetric and symmetric ionic liquid series, reflecting a decrease in the electrostatic interactions between the ionic species arising from the decrease of charge accessibility between the ionic pairs (ethyl and a propyl group connected to the positions 1 and 3 of the cation). That is in agreement with the decrease of the $\Delta_l^g H_m^o$ from [C$_1$C$_1$im][NTf$_2$] > [C$_2$C$_1$im][NTf$_2$] > [C$_2$C$_2$im][NTf$_2$] discussed above.

Acknowledgments

References

[1] M.A.A. Rocha, C.F.R.A.C. Lima, L.R. Gomes, B. Schröder, J.A.P. Coutinho, I.M. Marrucho, J.M.S.S. Esperança, L.P.N. Rebelo, K. Shimizu, J.N. Canongia Lopes, L.M.N.B.F. Santos, J. Phys. Chem. B 115 (2011) 10919.

[2] K. Shimizu, M.F. Costa Gomes, A.A.H. Pádua, L.P.N. Rebelo, J.N. Canongia Lopes, J. Mol. Struct. – THEOCHEM 946 (2010) 70.

[3] M.A.A. Rocha, J.A.P. Coutinho, L.M.N.B.F. Santos, J. Phys. Chem. B 116 (2012) 10922.

[4] M.A.A. Rocha, M. Bastos, J.A.P. Coutinho, L.M.N.B.F. Santos, J. Chem. Thermodyn. 53 (2012) 140.

[5] L.M.N.B.F. Santos, L.M.S.S. Lima, C.F.R.A.C. Lima, F.D. Magalhães, M.C. Torres, B. Schröder, M.A.V. Ribeiro da Silva, J. Chem. Thermodyn. 43 (2011) 834.

[6] P.L. Short, Chem. Eng. News 84 (2006) 15.

[7] M. Freemantle, Chem. Eng. News 85 (2007) 23.

[8] http://www.sigmaaldrich.com/chemistry/chemical-synthesis/technology-spotlights/cbils.html.

[9] M.E. Wieser, M. Berglund, Pure Appl. Chem. 81 (2009) 2131–2156.

[10] E.C.W. Clarke, D.N. Glew, Trans. Faraday Soc. 62 (1966) 539.

[11] P.J. Mohr, B.N. Taylor, D.B. Newell, Rev. Mod. Phys. 84 (2012) 1527.

[12] Y.U. Paulechka, G.J. Kabo, V.N. Emel'yanenko, J. Phys. Chem. B 112 (2008) 15708.

[13] A.V. Blokhin, Y.U. Paulechka, G.J. Kabo, J. Chem. Eng. Data 51 (2006) 1377.

[14] Y.U. Paulechka, A.V. Blokhin, G.J. Kabo, A.A. Strechan, J. Chem. Thermodyn. 39 (2007) 866.

[15] A.V. Blokhin, Y.U. Paulechka, A.A. Strechan, G.J. Kabo, J. Phys. Chem. B 112 (2008) 4357.

[16] D.H. Zaitsau, G.J. Kabo, A.A. Strechan, Y.U. Paulechka, A. Tschersich, S.P. Verevkin, A. Heintz, J. Phys. Chem. A 110 (2006) 7303.

[17] A.M. Fernandes, M.A.A. Rocha, M.G. Freire, I.M. Marrucho, J.A.P. Coutinho, L.M.N.B.F. Santos, J. Phys. Chem. B 115 (2011) 4033.

JCT 13-328